

Formation of negative ions *via* resonant low-energy electron capture by cysteine and cystine methyl esters

M. V. Muftakhov,* P. V. Shchukin, R. V. Khatymov, and R. F. Tuktarov

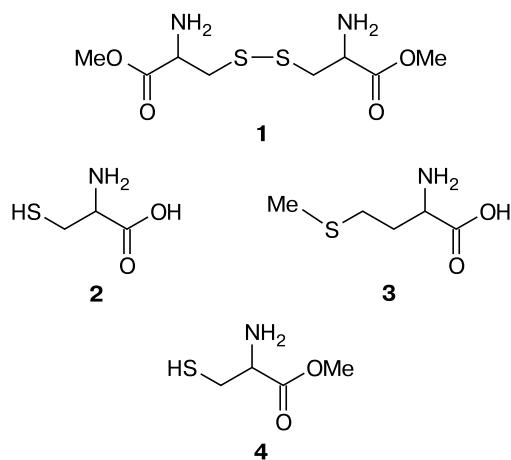
Institute of Molecule and Crystal Physics, Ufa Research Center of the Russian Academy of Sciences,
151 prosp. Oktyabrya, 450075 Ufa, Russian Federation.
Fax: +7 (347) 235 9522. E-mail: LMSNI@anrb.ru

The processes of resonance low-energy free electron attachment to methyl esters of some sulfur-containing amino acids were studied. The long-lived molecular negative ions of cystine dimethyl ester formed in the valence state *via* the Feshbach nuclear excited resonance mechanism were detected by mass spectrometry. The reactions of disulfide bond dissociation were identified in an electron energy range of 0–1 eV. They can be considered as model reactions regarding processes of peptide decomposition due to the resonance interaction with low-energy electrons. Predissociation of short-lived molecular ions of cysteine methyl ester formed by capture of electrons with energies of ~1.6 eV is accompanied by the intra-ionic transfer of negative charge from the carbonyl group to the sulfur atom leading to the elimination from the latter of hydrogen atom.

Key words: mass spectrometry, resonant electron capture, negative ions, cysteine methyl ester, cystine dimethyl ester, charge transfer.

Significant interest in studying negative ions (NI) of amino acids is due to the fact that they are building blocks of protein macromolecules playing the key role in processes of living activity of organisms. To the present time, mechanisms of extra-electron attachment to molecules of some aliphatic,^{1–7} aromatic,⁷ and heterocyclic^{7–10} amino acids have been established and the main channels of decomposition of molecular negative ions ($M^{-\bullet}$) have been revealed. However, the study of reactions involving NI of amino acids only does not provide exhaustive information about the processes in protein molecules during their interaction with low-energy electrons. Earlier, to elucidate this problem, we carried out a cycle of studies of larger di- and tripeptides^{11–14} consisting of amino acid residues of glycine and alanine. It was mentioned among the main conclusions that the decomposition of the aliphatic polypeptide chain in the ionized form of proteins can proceed as a simple cleavage of central (peptide, C–C and N–C α) bonds. The next step in this route is the study of electron-induced decomposition of disulfide bonds in the polypeptide and protein structures. For this purpose, cystine, the molecule of which consists of two cysteine residues linked by the disulfide bridge, was primarily assumed to be used as a model object. However, it is difficult to study cystine by mass spectrometry of resonant electron capture because of the thermocatalytic decomposition of the sample in the course of its sublimation on heating. Therefore, in this work we used cystine dimethyl ester (**1**), since methyl esters of amino acids have low vaporization temperatures.¹⁵

Cysteine (**2**), methionine (**3**), and cysteine methyl ester (**4**) served as auxiliary compounds.



Experimental

Experiments were carried out on a MI-1201V magnetic sector mass spectrometer (Ukraine, Sumy) modified for the operation with NI.¹⁶ The electronic energy scale was calibrated using $SF_6^{-\bullet}$ / SF_6 (~0 eV) and $[M - H]^{-\bullet}/MeCOOH$ (~1.55 eV).¹⁷ The procedure for determination of the cross section of fragmentation NI formation was described earlier.¹⁸

The average lifetime of NI relative to that of electron auto-detachment (τ_a) was determined in a mass spectrometric experiment using a previously described procedure.¹⁹ An additional

Table 1. Calculated enthalpies of formation of neutral and charged particles (ΔH_f° , eV) on the basis of which the threshold energies of formation of fragmentation negative ions were calculated

Particle A	ΔH_f° [A]	ΔH_f° [A ⁻]
$\cdot\text{SCH}_2\text{CH}(\text{NH}_2)\text{COOMe}$	-2.633	-4.966
$\text{HSCH}_2\text{CH}(\text{NH}_2)\text{COOMe}$	-3.990	-3.381
$\text{S}=\text{CHCH}(\text{NH}_2)\text{COOMe}$	-2.630	-3.621
$\text{MeOOCCH}(\text{NH}_2)\text{CH}_2\text{SSCH}_2\text{CH}(\text{NH}_2)\text{COOMe}$	-7.833	-8.947
$\cdot\text{H}$	2.261	—
MeSSMe	-0.328	—
MeS \cdot	1.185	-0.607
$\text{S}=\text{CH}_2$	—	0.690
MeSH	-0.200	—

electrode is mounted in the region of an ion receiver. A high potential application to this electrode resulted in a deviation of the charged component of the ion beam (I^-) in the cross electrical field, and neutrals (I^0) formed by electron autodetachment were detected by flight of ions of the field-free region after an analyzing magnet. Thus, the instrument makes it possible to detect either the total current of ions and neutral particles ($I^- + I^0$), or the current of neutral particles I^0 . The τ_a value is calculated from the equation

$$\tau_a = t / \ln(1 + I^0/I^-),$$

where t is the ion drift time in the field-free region of the instrument determined by the length of this region and the mass and kinetic energy of the ions. Commercial samples of the compounds (Sigma-Aldrich) were studied as received. A direct inlet tube was used for supplying vapor of the substance into the ionization chamber. The tube was heated to the temperature of optimum sublimation of the substance. A sample of cysteine (99%) was heated to 92 °C, methionine (98%) was heated to 135 °C, cysteine methyl ester (98%) was heated to 31 °C, and a sample of cystine dimethyl ester (95%) was heated to 80 °C. The temperature of the chamber was maintained at a level by 10–30° higher. The color of the samples remained non-consumed after experiment in the inlet tube was almost the same as the initial color, which indirectly indicated the absence of thermocatalytic decomposition on heating to the temperatures specified above.

Calculations. The energy threshold for dissociative reactions was calculated from the enthalpies of formation of neutral particles and ions (Table 1) obtained by the correction of the total energies of particles by the X1 neuron method.²⁰ The total energies of particles were calculated using the DFT method in the B3LYP hybrid functional in combination with the 6-311+G(d,p) basis set of atomic orbitals. Electron affinity was determined as the difference of the total energies of a neutral particle and ion calculated by the X1 method.

Results and Discussion

Resonant electron capture by cysteine^{21,22} and methionine²³ molecules was studied earlier. About ten types of NI were found for each object. A distinctive feature of these compounds compared to aliphatic amino acids con-

taining no sulfur atoms is the formation of a series of ions, for example, S^- and SH^- from cysteine, upon capture by the molecules of electrons of thermal and superthermal energies, which can be explained by exothermicity of the processes. However, no exhaustive explanation was found for the fact of efficient formation of ions with m/z 71 ($[\text{M} - (\text{NH}_3 + \text{H}_2\text{S})]^-$) from cysteine and m/z 83 ($[\text{M} - (\text{MeSH} + \text{H}_2\text{O})]^-$) from methionine in this energy range.^{21,23} At least ten low-intensity ion peaks were observed additionally in this work in the mass spectra of these compounds due to a higher sensitivity of the instrument used, but a reason for the formation of some of them in the low-energy range remained yet unclear.

Processes of NI formation from cysteine methyl ester were not studied earlier. Our experiment showed that the fragmentation of short-lived molecular ions occurs in the electron energy range 0–12 eV and is characterized by a smaller number of channels than in cysteine and methionine. The major peak in its mass spectrum corresponds to $[\text{M} - \text{H}]^-$ ions and the intensity of other peaks, the majority of which is observed in a low-energy range below 1 eV, does not exceed 2% (except for ions S^- and SH^-). Resonant electron capture by cystine dimethyl ester molecules is also studied for the first time. The peak with maximum intensity in its spectrum corresponds to ions with m/z 133, the intensity of other peaks is low as in the previous object, and the most part of them is detected in the low-energy range.

Ions $[\text{M} - \text{H}]^-$. No $[\text{M} - \text{H}]^-$ ions were found for cystine dimethyl ester. The effective output curves of $[\text{M} - \text{H}]^-$ ions from methionine, cysteine, and its methyl ester, which are formed in the range of energies not higher than 4.5 eV, are presented in Fig. 1. The cross sections of their formation are of the same order as $[\text{M} - \text{H}]^-$ ions in the mass spectra of aliphatic amino acids in the range of low energies ($\sim 10^{-18}$ cm²).¹¹ The resonance peaks of ions from methionine and cysteine ester are comparatively narrow and are remote by 0.5 eV in the electron energy scale. The resonance peak of cysteine is somewhat broadened and its maximum lies between the peak maxima of me-

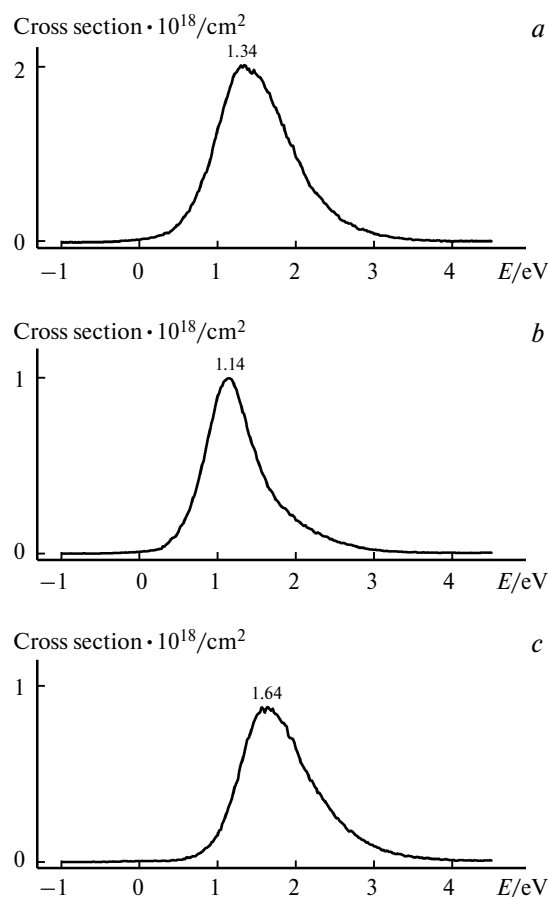
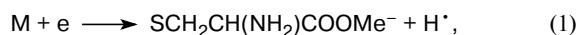


Fig. 1. Effective output curves for $[M - H]^-$ ions from cysteine (a), methionine (b), and cysteine methyl ester (c) ($\Delta E_{1/2} \sim 0.5$ eV). Digits in the curves designate maximum energy values.

thionine and cysteine ester, indicating the possibility of superposition of two peaks from methionine and ester.

It should be noted that, according to published results,¹⁵ the short-lived molecular ions from glycine in the low-energy range are formed *via* mechanisms of vibration-excited resonance (ions in the dipole-bound state) and single-particle shape resonance (ions in the valence state with one electron on the lowest vacant molecular orbital π_{OO}^*). These two states decompose *via* predissociation to $[M - H]^-$ ions due to the ejection of hydrogen atom of the carboxyl group. The dipole-bound state $M^{\bullet-}$ appears in the output curve of fragmentation ions as a narrow peak (of the fine vibration structure) from the side of lower energies, and the valence state appears as a broad peak from the side of higher energies, which explains the nonsymmetric shape of the curve. The origin of the $[M - H]^-$ ions from methionine is similar. The experiment with this object was carried out²³ with the best resolution by electron energy ($\Delta E_{1/2} = 0.15$ eV). The regions corresponding to the mentioned two resonance states are well discernible in the ion output curve and intersect at an energy of ~ 1.6 eV.

On going to cysteine ester, we can conclude that $[M - H]^-$ ions are formed from the ester *via* decomposition of the valence resonance state $^2[\pi_{OO}^*]$ only. These ions are evidently formed due to S—H bond dissociation, which is confirmed by the calculation of the energy of ion appearance (AE) using the equation of energy balance of the reaction using thermochemical constants of the ions, molecules, and radicals from Table 1



$$\text{AE} = 1.28 \text{ eV.}$$

Thus, the output curve of ions from cysteine is caused by processes of carboxylic hydrogen atom ejection, which is impossible in the case of its methyl ester, and ejection of the hydrogen atom bound to the sulfur atom, which is impossible for methionine. The H—C $_{\alpha}$ bond can dissociate in a range of 3 eV,¹⁷ but this process is not almost observed in the ion output curves because of the small cross section. The formation of $[M - H]^-$ ions from cysteine methyl ester will be discussed in detail further.

The mechanism of predissociation of molecular negative ions was discussed in detail¹⁵ for glycine. In particular, it was asserted that the $^2[\pi_{OO}^*]$ state to dissociate with the formation of $[M - H]^-$ ions in the range >1.5 eV needs to interact with the decaying $^2[\sigma_{OH}^*]$ state, which occurs due to the involvement of appropriate vibration modes. Thus, the $^2[\pi_{OO}^*]$ shape resonance serves as an "inlet" state for fragmentation and the decaying state $^2[\sigma_{OH}^*]$ is "final." In the case of cysteine methyl ester, $^2[\sigma_{SH}^*]$ is the "final" state (Fig. 2). An additional electron should occupy the vacant molecular orbital σ_{SH}^* localized, according to the calculations, on the S atom and its nearest environment. The π_{OO}^* orbital is completely localized on the C=O double bond of the —COOMe group, *i.e.*, on another end of the molecule. The $>\text{C}=\text{O}$ carbonyl group is a strong electron acceptor. It is reasonable to assume that this group is the center of capture of the flying electron for the π_{OO}^* shape resonance. Unlike the mechanism of vibration-excited resonance, the appearance of the π^* shape resonance results in an insignificant change in the geometry of the molecular system, whereas the lifetime of the ion relative to electron ejection are determined by the transparency coefficient of the potential barrier through which the flying electron tunnels. The equilibrium geometry of the primarily formed $M^{\bullet-}$ ions changes with time due to vibrational motions of the atoms. The electron density distribution on atoms for these ions is shown in Fig. 3, a. Due to fluctuations, the vibration energy in the ion can be concentrated on the valence vibration mode of the S—H bond, resulting in its extension (see Fig. 3, b) and then in dissociation (see Fig. 3, c). Owing to S—H bond activation, the electron density in the molecular system is redistributed, which is observed as an increase in the excessive negative charge on the sulfur atom. There-

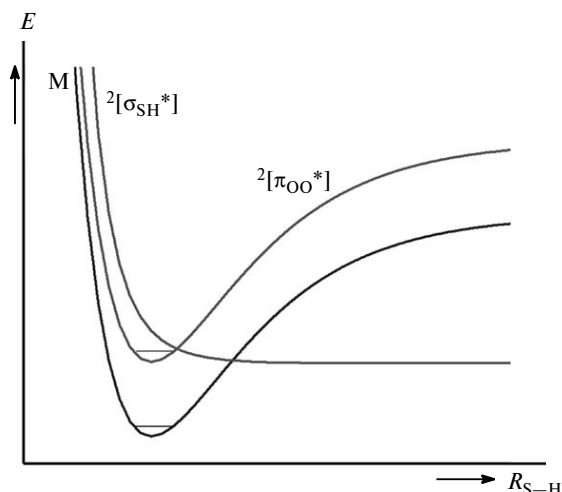


Fig. 2. Section of the potential energy surface of a neutral molecule (M) and a molecular ion in the π^* - and σ^* -states along the S—H bond illustrating the predissociative process of formation of $[M-H]^-$ ions in cysteine methyl ester.

fore, predissociation of the molecular ion illustrated in Fig. 2 is accompanied by the negative charge transfer inside the ion from the carbonyl group to the sulfur atom. The rate of charge transfer (the carrier of the transfer is the captured electron) depends on the duration of nonradiative transition between the $2[\pi_{OO}^*]$ and $2[\sigma_{SH}^*]$ states and ion size. Taking into account that the characteristic time of these transitions in molecular system is $<10^{-11}$ s, an approximate estimate of the minimum electron transfer rate in the ion gives ~ 50 m s $^{-1}$.

The electron density distribution on the $M^{\cdot-}$ at any moment depends on its spatial configuration, since the electronic subsystem is rapidly "tuned" to a new geometry even upon an insignificant shifts of atoms from their positions. In this respect, the S—H bond elongation is indicative. As the hydrogen atom remotes from the sulfur atom, a deficient of the negative charge is formed on the sulfur atom, and to compensate it, the S atom withdraws the electron density from the whole ion (*cf.* Figs. 3, *a* and *b*). Therefore, the decomposition of the S—H bond is not a necessary condition for the intra-ionic electron transfer, and its elongation is sufficient. This makes it possible to consider a molecule of cysteine ester as a electrical current carrier. An idea to use peptides (along with nucleic acids) for the production of nanowires in miniature organic electronic devices is discussed presently in scientific literature,^{24,25} and this concept is based, most likely, on the possibility of electron transfer between the adjacent peptide groups over the whole chain length.

Long-lived molecular ions of cystine dimethyl ester.

Molecular ions are observed fairly rarely in experiments on resonance electron capture, since they decompose, in most cases, already in the ionization chamber. Molecular ions formed *via* the Feshbach vibration-excited resonance

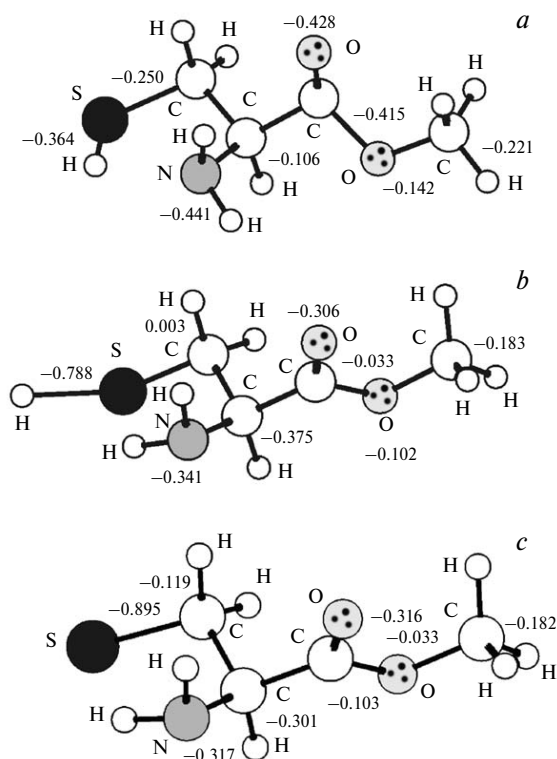


Fig. 3. Spatial geometry of negative ions from cysteine methyl ester calculated by the B3LYP/6-311+G(d,p) method indicating charge contributions on the heavy atoms (optimization over the total energy): *a*, M^- in the ground state; *b*, M^- in the ground state with the S—H bond twofold elongated compared to (*a*); and *c*, $[M-H]^-$ formed by S—H bond dissociation in the ground state.

mechanism by thermal energy electron capture are mainly detected using mass spectrometry. On the one hand, this is due to the relatively long lifetime of these ions with respect to autoneutralization. On the other hand, this is caused by a low energy introduced by an electron to the molecular system, which is insufficient for the initiation of dissociative processes. Dipole-bound states $M^{\cdot-}$ of amino acids, peptides, nitrous bases, and sugars are formed in the low-energy range by vibration-excited resonance but are characterized by a short lifetime with respect to electron ejection. Therefore, it is not surprising that peaks of $M^{\cdot-}$ were not observed in numerous studies of NI of these objects. We have recently²⁶ detected the peak of $M^{\cdot-}$ in the mass spectrum of uridine, and the purposeful search for similar ions in other nucleosides gave no results. The more so, the detection of the peak with m/z 268 corresponding to long-lived molecular ions in the mass spectrum of cystine dimethyl ester seems remarkable in the context of the aforesaid.

Molecular ions from cysteine ester are formed in the range of thermal energies and unstable relative to electron autodetachment. The effective output curves of these ions and their neutrals obtained at various temperatures are

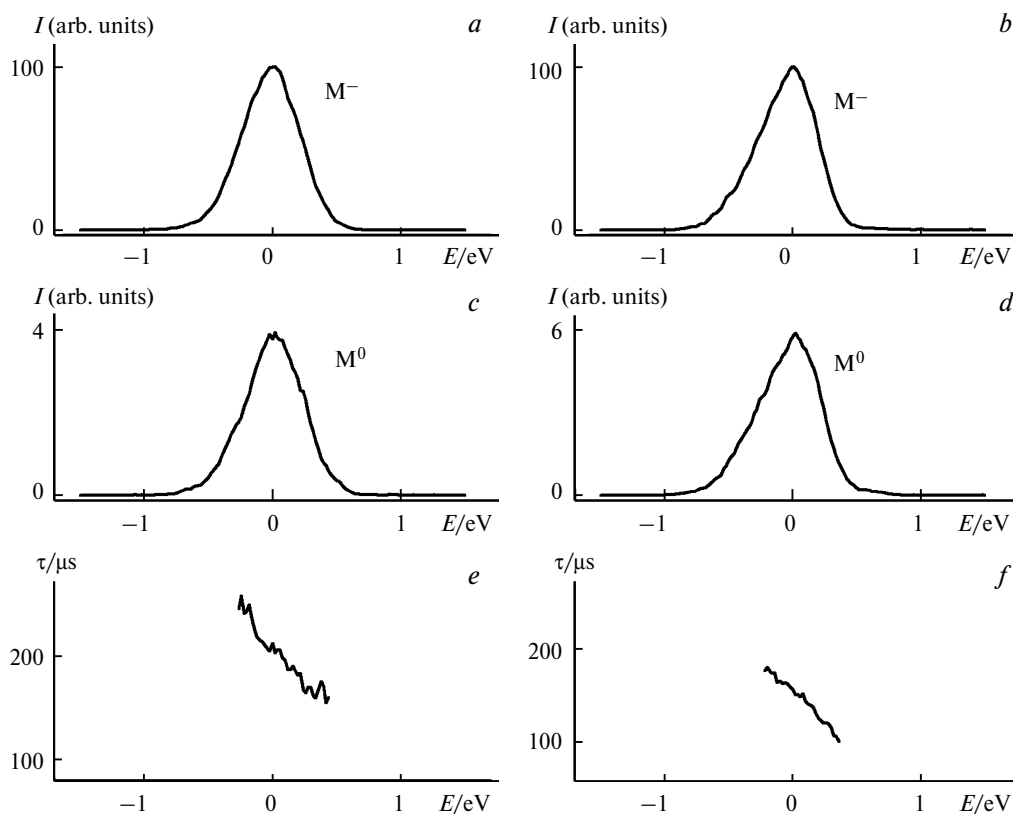


Fig. 4. Effective outputs of molecular ions (M^-) and their neutrals (M^0) from cystine dimethyl ester vs electron energy at the temperature of the chamber 84 (a, c) and 138 °C (b, d) ($\Delta E_{1/2} = 0.52$ eV). e, f. Lifetime of ions relative to electron autodetachment.

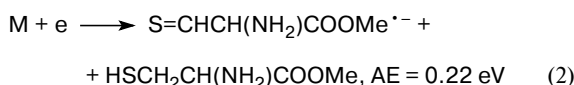
presented in Fig. 4. The dependences of the lifetime of ions as a function of the electronic energy are also shown in Fig. 4. The descending with energy character of this dependence indicates the "non-zero" resonance width and characterizes it as a vibration-excited resonance. The range of its abundance in the energy scale cannot be determined from the data obtained, but it was found that the output curves of the discussed ions are identical to those of $SF_6^{\cdot-}$ ions in terms of the experimental conditions.

The internal energy of $M^{\cdot-}$ ions increases with temperature (since they inherit the internal vibration energy of the molecules), inducing a more intense decomposition by electron autodetachment. This is manifested in experiment as a decrease in the absolute and relative intensities of the peaks of $M^{\cdot-}$ ions in the mass spectrum and a decrease in their lifetime. The fact of existence of this temperature dependence of τ_a indicates the statistical character of electron autodetachment. According to the Rice—Ramsperger—Kassel—Marcus (RRKM) Statistical theory, the rate constant of ion decomposition depends on their internal energy only. It is of no importance in which form it was obtained: in the form of the captured electron energy or thermal energy. This is also valid for τ_a , because this value is reciprocal toward the rate constant in sense. Therefore, the dependence of τ_a for different temperatures in the

internal energy scale of ions represents the same function. The scale of electron energy exhibits the shift along the horizontal by the difference of internal energies of neutral molecules at these temperatures.²⁷

The question about the nature of the resonance state of long-lived $M^{\cdot-}$ of cystine dimethyl ester is elucidated by the results of quantum chemical calculations. The adiabatic electron affinity of the molecule in the ground state is positive and exceeds 1 eV (see Table 1). The valence state of $M^{\cdot-}$ is formed by electron capture to the lowest unoccupied molecular orbital σ_{SS}^* localized in the disulfide bond. In spite of the fact that the lifetime of molecular ions relative to the captured electron ejection achieved hundreds of μ s, the relative intensity of the corresponding peak in the mass spectrum is low ($\sim 2\%$). Possibly, this is due to the intense fragmentation that takes place already at the thermal energy of electrons. In fact, the intensive output of ions with m/z 133 is observed in this energy range, and there are other, less intense channels of fragmentation (Fig. 5). We observed a similar case earlier when studying a series of *N*-derivatives of acridone,²⁸ whose mass spectra contained intense molecular peaks of $M^{\cdot-}$. An intensive channel of fragmentation was detected for one of the objects of the series, and the peak of M^- was not observed in the mass spectrum for this object.

Ions $\text{S}=\text{CHCH}(\text{NH}_2)\text{COOMe}^{\cdot-}$ and $\text{SCH}_2\text{CH}(\text{NH}_2)\text{COOMe}^-$ in cystine dimethyl ester. The most intense ions with m/z 133 are formed in an energy range of 0–1 eV with the maximum output at 0.16 eV (see Fig. 5). The calculation of different variants of structures of the ion and uncharged fragments of $\text{M}^{\cdot-}$ decomposition suggested the rearrangement mechanism of its formation as the least energy consuming (see Eq. (2)). Here the $\text{H}(\text{C}_\beta)$ atom migrates to the sulfur atom through the disulfide bond accompanied by the cleavage of this bond. The uncharged counterfragment of decomposition is a molecule of cysteine methyl ester.



According to the data on the abundance of isotopes of various elements, the ratio of intensities of isotope peaks

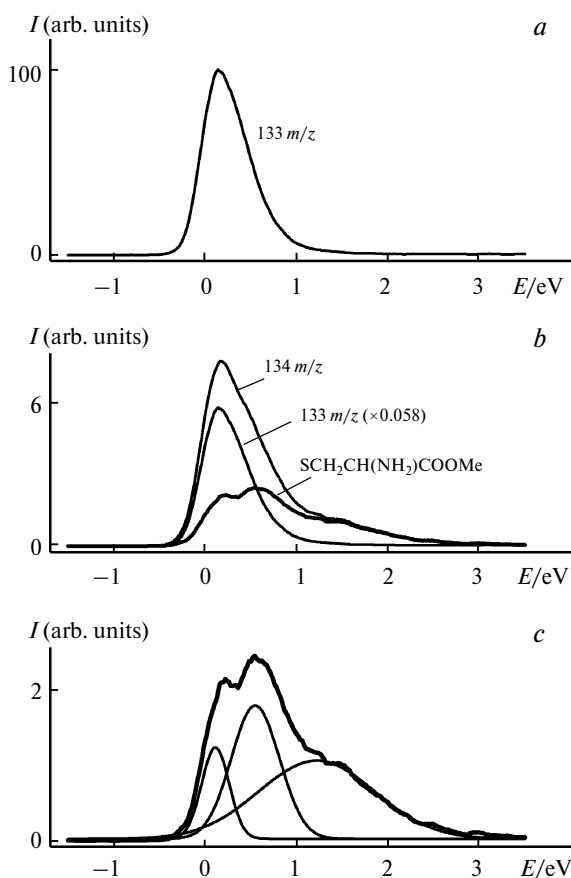
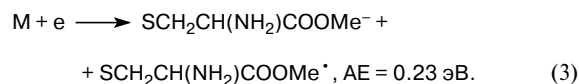


Fig. 5. Effective outputs of ions vs electron energy of cystine dimethyl ester ($\Delta E_{1/2} = 0.3$ eV): *a*, $\text{S}=\text{CHCH}(\text{NH}_2)\text{COOMe}^{\cdot-}$ ions (m/z 133); *b*, experimental curves for ion peaks with m/z 133 and 134 (thin lines) and as a result of their difference the output curve of $\text{SCH}_2\text{CH}(\text{NH}_2)\text{COOMe}^-$ ions (thick line); *c*, decomposition of the output curve of $\text{SCH}_2\text{CH}(\text{NH}_2)\text{COOMe}^-$ ions (thick line) over the Gaussian functions (thin lines), and the envelope is omitted.

of the discussed ion with m/z 133 and 134 should be 100 : 5.8, which is almost obeyed (100 : 7.5) in the mass spectrum recorded at a fixed energy of ~ 0 eV (see Fig. 5). At the same time, the discussed peaks are nearly equally intense in the mass spectrum at 1.5 eV, which indicates the existence of other ions with m/z 134, *i.e.*, containing the additional hydrogen atom. we concluded that the latter were formed by the simple cleavage of the disulfide bond



The individual effective output curve of $\text{SCH}_2\text{CH}(\text{NH}_2)\text{COOMe}^-$ ions isolated by the subtraction of the contribution of the isotope peak with m/z (133 + 1) of the $\text{S}=\text{CHCH}(\text{NH}_2)\text{COOMe}^{\cdot-}$ from the composite peak with m/z 134 is presented in Fig. 5, *b*. This curve makes it possible to preliminarily distinguish the main maximum in a range of 0.6 eV, a poorly resolved maximum in a range of 0.2 eV, and a shoulder at 1.3 eV. The obtained curve was examined more thoroughly through the decomposition procedure to the Gaussian functions. The analysis showed that the ion output curve consisted indeed of three overlapped resonance peaks (see Fig. 5, *c*). A broad peak at 1.3 eV isolated by this procedure is associated with the resonance state $\text{M}^{\cdot-}$ similar to the ${}^2[\pi_{\text{OO}}^*]$ state in cysteine methyl ester. The maximum at 0.2 eV corresponds to the vibration-excited ${}^2[\sigma_{\text{SS}}^*]$ shape resonance, and the maximum at 0.6 eV is the threshold process of formation of fragmentation ions from the single-particle ${}^2[\sigma^*]$ shape resonance. Therefore, it can be concluded for the $\text{S}=\text{CHCH}(\text{NH}_2)\text{COOMe}^{\cdot-}$ ions that they are also formed due to the decomposition of the ${}^2[\sigma_{\text{SS}}^*]$ and ${}^2[\sigma^*]$ states.

It is seen from the curves presented in Fig. 5 that the output of rearrangement ions is much more intense than the output of ions formed in the reaction of simple bond cleavage. At the first glance, this pattern contradicts the concepts about rearrangement processes, since they require more time and, hence, they should be suppressed strongly by the competitive electron autodetachment. At the same time, this contradiction can be explained is taking into account the differences in the energetics of the processes.

First, there can be barrier in the path of simple bond cleavage (activation energy of the backward reaction), which requires an additional energy to surmount it. In the rearrangement process, the molecular system has a sufficient time to "walk around" this barrier without attracting an additional energy to surmount it. Attempts to calculate the form of the potential energy surface in the section along the reaction coordinate (S—S bond extension) did not give unambiguous results, which can be interpreted as the absence of the barrier or a restricted possibility of the applied methods that does not allow its detection.

Second, a lower threshold energy can be assumed for the rearrangement process, which would provide an advan-

tage over the simple bond cleavage. Our calculations confirm this in part, but the difference in threshold energies turned out to be very small, only 0.01 eV (*cf.* Eqs (2) and (3)), which can be caused, however, by inaccuracies of calculations.

In the framework of the discussed problem, we analyzed the results of Ref. 29 in which we were interested in $S=CH_2^{\cdot-}$ and SMe^- ions from CH_3SSMe having the structure identical to the $S=CHCH(NH_2)COOMe^{\cdot-}$ and $SCH_2CH(NH_2)COOMe_3^-$ ions and formed in similar processes



The effective output curves are symmetric cupola-like peaks of approximately equal widths, and the intensity of the signal of $S=CH_2^{\cdot-}$ is by 2.5 times higher than the intensity of SMe^- . The peak maxima are detected at 0.67 and 0.86 eV, respectively,²⁹ they are remote from each other at 0.19 eV. The beginnings of the peaks are remote at approximately the same value, which by ~0.1 eV exceeds the calculated difference between the AE of ions (0.09 eV, *cf.* Eqs (4) and (5)). Thus, it is quite probable that the threshold energies of processes (2) and (3) can also differ by a more significant value of 0.1–0.2 eV than the calculated difference equal to 0.01 eV.

Thus, the light and mobile carboxylic hydrogen atom plays an important role in low-energy electron-molecular resonance interactions with the formation of negative ions of amino acids and simplest peptides. In particular, processes of H atom detachment or migration to form ions of the $XCOO^-$ type are most intensive, and it is rather difficult to detect other, less intensive decomposition process without participation of this atom against their background. As mentioned earlier,¹⁵ amino acid derivatization and the work with their esters give an additional advantage along with the decrease in the vaporization temperature, which makes it possible to reveal these fragmentation channels. Among them are the channel of formation of $[M - H]^-$ ions by S–H bond dissociation in cysteine methyl ester, which poorly discernible in cysteine.²¹ Unlike the formation of ion with the carboxyl structure, this reaction exemplifies a process with charge transfer inside the ions and can be significant for the simulation of phenomena related to electron transfer in polypeptides.

The protein macrostructure is caused by the formation of various types of bonds between the amino acid fragments of the polypeptide chain. The decomposition of these bonds results in protein denaturation and the loss of its original properties. Disulfide bonds occupy a special place among them. For example, hormones oxytocin, vasopressin, and insulin hormones interesting from the

medical point of view lose biological activity when the disulfide bond is decomposed. The decomposition of these bonds in an aqueous medium can occur in the presence of oxidants or reducing agents. As shown by the results of experiments with NI of cystine dimethyl ester, solvated electrons characterized by low energies can play a similar role. In this context, the reactions of isolation of $S=CHCH(NH_2)COOMe^{\cdot-}$ and $SCH_2CH(NH_2)COOMe^-$ ions can be considered as model reactions in polypeptides.

References

1. S. Gohlke, A. Rosa, E. Illenberger, F. Brüning, M. A. Huels, *J. Chem. Phys.*, 2002, **116**, 10164.
2. S. Ptasínska, S. Denifl, P. Candori, S. Matejcik, P. Scheier, T. D. Märk, *Chem. Phys. Lett.*, 2005, **403**, 107.
3. P. Papp, J. Urban, S. Matejcik, M. Stano, O. Ingolfsson, *J. Chem. Phys.*, 2006, **125**, 204301.
4. S. Denifl, H. D. Flosadyttir, A. Edtbauer, O. Ingylfsson, T. D. Märk, P. Scheier, *Eur. Phys. J.*, 2010, **60**, 37.
5. P. Papp, P. Shchukin, S. Matejcik, *J. Chem. Phys.*, 2010, **132**, 014301.
6. J. Kocisek, P. Papp, P. Mach, Y. V. Vasil'ev, M. L. Deinzer, S. Matejcik, *J. Phys. Chem. A*, 2010, **114**, 1677.
7. Y. V. Vasil'ev, B. J. Figard, V. G. Voinov, D. F. Barofsky, M. L. Deinzer, *J. Am. Chem. Soc.*, 2006, **128**, 5506.
8. H. Abdoul-Carime, E. Illenberger, *Chem. Phys. Lett.*, 2004, **397**, 309.
9. P. Sulzer, E. Alizadeh, A. Mauracher, T. D. Märk, P. Scheier, *Int. J. Mass Spectrom.*, 2008, **277**, 274.
10. H. Abdoul-Carime, S. Gohlke, E. Illenberger, *Chem. Phys. Lett.*, 2005, **402**, 497.
11. M. V. Muftakhov, P. V. Shchukin, *Russ. Chem. Bull. (Int. Ed.)*, 2010, **50**, 896 [*Izv. Akad. Nauk, Ser. Khim.*, 2010, 875].
12. M. V. Muftakhov, P. V. Shchukin, *Phys. Chem. Chem. Phys.*, 2011, **13**, 4600.
13. P. V. Shchukin, M. V. Muftakhov, A. V. Pogulay, *Rapid Commun. Mass Spectrom.*, 2012, **26**, 828.
14. M. V. Muftakhov, P. V. Shchukin, *Russ. Chem. Bull. (Int. Ed.)*, 2014, **63**, 642 [*Izv. Akad. Nauk, Ser. Khim.*, 2014, 642].
15. Y. V. Vasil'ev, B. J. Figard, D. F. Barofsky, M. L. Deinzer, *Int. J. Mass Spectrom.*, 2007, **268**, 106.
16. V. A. Mazunov, P. V. Shchukin, R. V. Khatymov, M. V. Muftakhov, *Mass-spektrometriya [Mass Spectrometry]*, 2006, **3**, 11 (in Russian).
17. M. V. Muftakhov, Yu. V. Vasil'ev, V. A. Mazunov, *Rapid Commun. Mass Spectrom.*, 1999, **13**, 1104.
18. R. V. Khatymov, M. V. Muftakhov, V. A. Mazunov, *Rapid Commun. Mass Spectrom.*, 2003, **17**, 2327.
19. D. Edelson, J. E. Griffiths, K. B. McAfee, *J. Chem. Phys.*, 1962, **73**, 919.
20. J. Wu, X. Xu, *J. Chem. Phys.*, 2007, **127**, 214105.
21. H. Abdoul-Carime, S. Gohlke, E. Illenberger, *Phys. Chem. Chem. Phys.*, 2004, **6**, 161.
22. K. Aflatoon, B. Hitt, G. A. Gallup, P. D. Burrow, *J. Chem. Phys.*, 2001, **115**, 6489.

23. J. Kopyra, I. Szamrej, H. Abdoul-Carime, B. Farizonbc, M. Farizon, *Phys. Chem. Chem. Phys.*, 2012, **14**, 8000
24. B. J. Pepe, R. Fairman, *Curr. Opin. Struct. Biol.*, 2009, **19**, 483.
25. Y. S. Yew, G. Shekhawat, N. Wangoo, S. Mhaisalkar, C. R. Suri, V. P. Dravid, Y. M. Lam, *Nanotechnology*, 2011, **22**, 215606.
26. M. V. Muftakhov, P. V. Shchukin, *J. Anal. Chem.*, 2013, **68**, 1200 [*Mass Spectrometry*, 2013, **10**, 39].
27. Yu. V. Vasil'ev, R. R. Abzalimov, S. K. Nasibullaev, T. Drevello, *Fullerene, Nanotubes and Carbon Nanostructures*, 2004, **12**, 229.
28. M. V. Muftakhov, Yu. V. Vasil'ev, R. V. Khatymov, V. A. Mazunov, V. V. Takhistov, O. V. Travkin, E. V. Yakovleva, *Rapid Commun. Mass Spectrom.*, 1999, **13**, 912.
29. A. Modelli, D. Jones, G. Distefano, M. Tronc, *Chem. Phys. Lett.*, 1991, **181**, 361.

*Received March 16, 2015;
in revised form October 19, 2015*